Modeling of magnetic island formation in magnetic reconnection experiment

journal or publication title	Physics of plasmas
volume	Vol.6
number	No.4
page range	pp.1253-1257
year	1999-04-01
URL	http://hdl.handle.net/10655/2283

doi: 10.1063/1.873368

Creative Commons : 表示 - 非営利 - 改変禁止
http://creativecommons.org/licenses/by-nc-nd/3.0/deed.ja

Modeling of magnetic island formation in magnetic reconnection experiment

T.-H. Watanabe, T. Hayashi, and T. Sato
Theory and Computer Simulation Center, National Institute for Fusion Science, Toki, Gifu, 509-5292, Japan

M. Yamada and H. Ji
Plasma Physics Laboratory, Princeton University, Princeton, New Jersey 08543

(Received 13 October 1998; accepted 12 January 1998)

Formation of a magnetic island found in the Magnetic Reconnection Experiment (MRX) [M. Yamada, H. Ji, S. Hsu, *et al.*, Phys. Plasmas **4**, 1936 (1997)] is investigated by a magnetohydrodynamic (MHD) relaxation theory and a numerical simulation. In the cohelicity injection with a mean toroidal field, the growing process of the island into a spheromak-type configuration is explained by quasistatic transition of the force-free and minimum energy state to a state with larger normalized helicity. It also turns out that no magnetic island would be generated in the counterhelicity case. The MHD simulation with inhomogeneous electric resistivity agrees with experimental results, which clearly shows formation and growth of the magnetic island in a diffusion region where the reconnection takes place. © *1999 American Institute of Physics.* [S1070-664X(99)03904-X]

I. INTRODUCTION

Magnetic reconnection has been regarded as one of the most important and fundamental processes in macroscopic phenomena in fusion, space, and astrophysical plasmas.[1–3] It is accepted that reconnection produces two significant effects, namely, the topological change of field lines and the conversion of energy. In the reconnection process, the released magnetic energy is converted into kinetic and thermal energies, resulting in acceleration and heating of the plasma. The topological change of field lines allows the plasma and magnetic field to relax towards a lower energy state characterized with a different topology.[4]

Recently, experimental studies of magnetic reconnection in magnetohydrodynamic (MHD) plasmas have been initiated by using coalescence of spheromaks,[5] where two types of operation mode have been pursued. One is a cohelicity merging using two identical spheromaks. The another one is a counterhelicity merging where toroidal fields in spheromaks are antiparallel. In a sequence of experiments, it was found that a field-reversed configuration (FRC) is obtained when the counterhelicity merging occurred through reconnection, whereas a spheromak is formed in the cohelicity case. A MHD simulation of the spheromak merging has confirmed the spontaneous FRC formation with effective plasma heating by magnetic reconnection.[6]

In the Magnetic Reconnection Experiment (MRX),[7] reconnection is examined as an elementary process in a plasma under a controlled condition, where a pair of flux-core (FC) coils with time-varying electric current inductively changes the field configuration to cause a plasma flow. The induced plasma flow drives the magnetic reconnection at the separatrix point (X-point). Two types of injection mode of a toroidal field (TF) are also available in the MRX, namely, co- and counterhelicity injections. Yamada and co-workers have found O-point formation during the magnetic reconnection in the cohelicity injection of the ''pull'' operation mode, where poloidal field (PF) coil currents are decreased in time. The O-point formed in the reconnection region grows like a spheromak.[8,9] In the counterhelicity case, on the other hand, a Y-shaped current sheet is formed when the magnetic reconnection takes place.

By means of MHD simulations using an adaptive mesh refinement technique, Schnack[10] has found formation of a small island during the null-helicity injection with no toroidal field, although it is unstable to motion along the current sheet and cannot grow stably.

In this paper, we report an investigation of the formation and growth mechanism of the magnetic island in the cohelicity injection of MRX. Since the MRX plasma has low temperature, its magnetic field would be approximately force-free. The Taylor state[11] in a rectangular container with a pair of FC coils is analyzed in the next section, which will suggest a plausible explanation to the island growth. Results of the MHD simulations and conclusions are given in Secs. III and IV, respectively.

II. TAYLOR STATES IN THE MRX CONFIGURATION

In this study we employ a MHD model of the MRX plasma, neglecting toroidal effects. A rectangular plasma container is taken to be a perfect conductor bounding the poloidal plasma domain of $-L_x \leqslant x \leqslant L_x$ and $-L_y \leqslant y \leqslant L_y$. We have assumed symmetry in z (toroidal) direction. Since no center rod is used in the MRX, one of the side boundaries at $x = \pm L_x$ corresponds to the major (symmetry) axis in comparison of the model configuration with the MRX device. Hereafter, we define $L_x = 1$ as a unit of length. L_y is set to be 1.4. A pair of FC coils with their radii of 0.2 are, respectively, placed at $(x,y) = (0, \pm 0.6)$. In order to accurately im-

 © 1999 American Institute of Physics

Downloaded 12 Jun 2009 to 133.75.139.172. Redistribution subject to AIP license or copyright; see http://pop.aip.org/pop/copyright.jsp

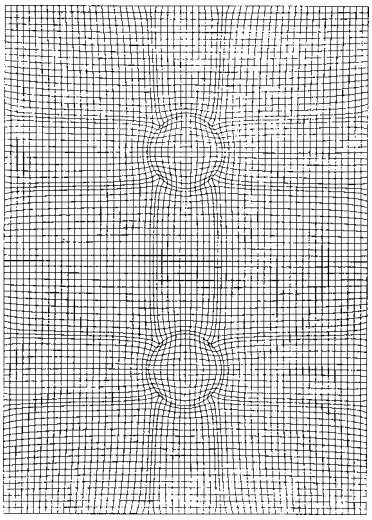

FIG. 1. An example of numerical grids in generalized curvilinear coordinates used in computation.

pose boundary conditions on the FC coils, we have used numerical grid points in generalized curvilinear coordinates as shown in Fig. 1.

First, we consider a case of the cohelicity injection. In a system with symmetry in z direction, a vector potential $\mathbf{A}$ can be given by

$$\mathbf{A}=\Psi\hat{\mathbf{z}}+\nabla H\times\hat{\mathbf{z}}, \tag{1}$$

where Ψ and H are scalar functions. Ψ means the so-called poloidal flux, although Eq. (1) involves freedom of a gauge potential. The magnetic field and the current density are, respectively,

$$\mathbf{B}=-\nabla^2 H\hat{\mathbf{z}}+\nabla\Psi\times\hat{\mathbf{z}} \tag{2}$$

and

$$\mathbf{j}=-\nabla^2\Psi\hat{\mathbf{z}}-\nabla(\nabla^2 H)\times\hat{\mathbf{z}}. \tag{3}$$

Substituting Eqs. (2) and (3) into the force-free equation of the Taylor state, $\mathbf{j}+\mu\mathbf{B}=0$, one finds that

$$\nabla^2\Psi=-\mu\nabla^2 H \tag{4}$$

and

$$\nabla(\nabla^2 H)=\mu\nabla\Psi. \tag{5}$$

Integration of Eq. (5) leads to

$$\nabla^2 H=\mu\Psi+C, \tag{6}$$

where C giving the vacuum toroidal field for $\mu=0$ should be determined so that a constant gauge potential X cannot influence on the left-hand side. In other words, for a gauge transformation of $\Psi\rightarrow\Psi+X$, C must be transformed as $C\rightarrow C-\mu X$, because $\nabla^2 H$, namely, B_z is gauge invariant. Since no external TF coil is used in the MRX device, one can choose $C=0$ when $\Psi=0$ on the container wall (outer boundary). It leads to

$$\nabla^2\Psi+\mu^2\Psi=0. \tag{7}$$

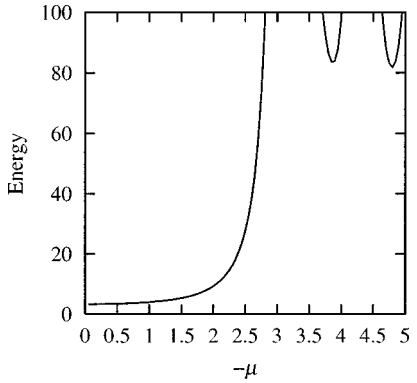

FIG. 2. Magnetic energy vs μ of the Taylor state with $\Psi_0=1$.

A boundary condition on the FC coil surfaces is given by $\Psi=\Psi_0=$constant.[12] One may set $\Psi_0=1$ without loss of generality, since Ψ_0 is used just to determine the amplitude of Ψ. Let us define $\tilde{\Psi}\equiv\Psi-\Psi_v$, where the poloidal flux of a vacuum field Ψ_v is calculated from $\nabla^2\Psi_v=0$ with $\Psi_v=0$ and Ψ_0 on the outer and inner boundaries. Therefore, $\tilde{\Psi}$ is a solution of

$$\nabla^2\tilde{\Psi}+\mu^2\tilde{\Psi}=-\mu^2\Psi_v \tag{8}$$

satisfying $\tilde{\Psi}=0$ on both the boundaries. Solving Eqs. (7) or (8) for given μ and Ψ_0, one finds a Taylor state in the model of MRX.

According to Taylor,[13] the magnetic helicity in a torus is defined as $K=\int\mathbf{A}\cdot\mathbf{B}dv-\oint\mathbf{A}\cdot d\mathbf{l}\oint\mathbf{A}\cdot d\mathbf{s}$ so that K is indeed invariant to a multivalued gauge potential χ. Here, $d\mathbf{l}$ and $d\mathbf{s}$ denote loop integrals the long and short way around the toroidal surface. In the model configuration of MRX, the gauge-invariant helicity is written as follows:

$$K\equiv\int\mathbf{A}\cdot\mathbf{B}dxdy-\sum_i\Psi_0\oint\mathbf{A}\cdot d\mathbf{l}_i, \tag{9}$$

where $d\mathbf{l}_i$ means the loop integral around the ith FC coil surface, while $dxdy$ denotes the integral in the multiply-connected region between the outer and inner boundaries. Substituting Eqs. (1) and (2) into Eq. (9), after some manipulation using Gauss theorem, one finds

$$K=-2\int\Psi\nabla^2 Hdxdy \tag{10}$$

when $\Psi=0$ and Ψ_0 on outer and inner boundaries. Calculation of the magnetic energy E is straightforward, that is,

$$E\equiv\frac{1}{2}\int B^2dxdy=\frac{1}{2}\int\{(\nabla^2 H)^2+(\nabla\Psi)^2\}dxdy. \tag{11}$$

We have numerically solved Eq. (7) by the second-order finite difference and the conjugate-gradient method, calculating E and K. The numerical solutions are shown in Figs. 2 and 3. Here, μ is set to be negative so that Ψ_0 and K are positive. Figure 2 shows that the energy increases with $|\mu|$, when $|\mu|$ is less than the lowest eigenvalue λ_1 of $\nabla^2 f_m+\lambda_m^2 f_m=0$ (Ref. 14) ($\lambda_1\simeq 3.2$ in the present case). This is because $\tilde{\Psi}$ satisfying Eq.(8) becomes much larger than Ψ_v

Downloaded 12 Jun 2009 to 133.75.139.172. Redistribution subject to AIP license or copyright; see http://pop.aip.org/pop/copyright.jsp

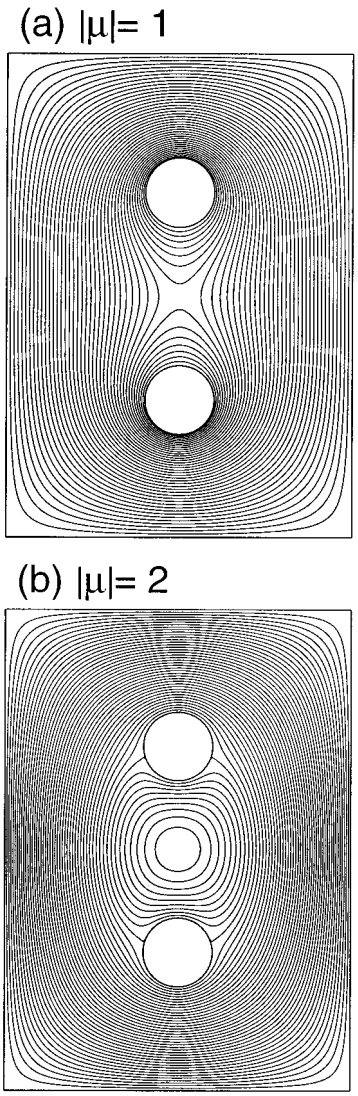

FIG. 3. Contour plots of poloidal flux for (a) $|\mu|=1$ and (b) 2.

as $|\mu|$ approaches to λ_1, where $\tilde{\Psi}$, as well as Ψ, is approximate to the lowest eigenfunction f_1. During $|\mu|$ is increased from 0 to λ_1, therefore, a magnetic island due to $\tilde{\Psi}$ appears and grows. Contour plots of Ψ for $|\mu|=1$ and 2 in Fig. 3 clearly shows a topological change of the Taylor state due to appearance of a magnetic island at the center of the system. The magnetic island becomes visible for $|\mu|>1.6$. As $|\mu|$ approaches to λ_1 further, the island with a spheromak-like configuration grows and finally covers the whole system.

In the cohelicity injection, the MRX plasma before decreasing the PF coil current may be approximate to a solution of Eq. (7) for $|\mu|<1.6$. As the PF coil current is reduced in a time scale longer than the Alfvén transit time, Ψ is ''pulled'' into the FC coils, namely, Ψ_0 becomes smaller. By short-circuiting the TF coil, toroidal flux would be conserved. This means that more plasma current is induced in the system, namely, $|\mu|$ is increased by decreasing Ψ [see Eq. (6)]. Thus, the energy and helicity, respectively, normalized by $(\Psi_0/L_x)^2$ and Ψ_0^2/L_x are increased. According to the Taylor state analysis given above, therefore, when $|\mu|>1.6$, the magnetic island will appear and grow spontaneously during the pulling operation with the cohelicity injection.

The Taylor state analysis also suggests that no magnetic island is formed in the counterhelicity injection. The reason is that, in the MRX configuration, there is no Taylor state having antisymmetry with respect to $y=0$. Since Ψ_v, namely, the PF current in the FC coils is assumed to be symmetric, $\tilde{\Psi}$, therefore, Ψ and B_z should be symmetric in y for $\mu\neq\lambda_m$. Extending the definition of the Taylor state with a constant μ, thus, one may consider an antisymmetric μ profile, which has opposite signs in $y>0$ and $y<0$, so that B_z could be antisymmetric for any symmetric Ψ. A possible configuration with the antisymmetric μ is as follows: The toroidal current j_z flows only in the ''private'' region inside of the figure-eight separatrix magnetic surface, while $j_z=0$, namely, $\mu=0$ in the ''public'' region outside of the separatrix surface. This is because j_z is a flux function [see Eqs. (3) and (7)]. Even if μ is antisymmetric, therefore, no magnetic island with a mean toroidal current is formed in the counterhelicity case for $|\mu|<\lambda_1$.

III. MHD SIMULATION OF MRX DISCHARGE

In order to check the prediction for the magnetic island formation in the last section, we have performed two-dimensional MHD simulations with the initial condition given by the Taylor state of $\mu=-1$ and $\Psi_0=1$, and have examined a time evolution of the system, with slowly decreasing Ψ_0 in time. Governing equations are as follows:

$$\frac{\partial\rho}{\partial t}=-\nabla\cdot(\rho\mathbf{v}), \tag{12}$$

$$\rho\frac{d\mathbf{v}}{dt}=-\nabla p+\mathbf{j}\times\mathbf{B}+\nu\left(\nabla^2\mathbf{v}+\frac{1}{3}\nabla(\nabla\cdot\mathbf{v})\right), \tag{13}$$

$$\frac{1}{\Gamma-1}\frac{dp}{dt}=-\frac{\Gamma}{\Gamma-1}p\nabla\cdot\mathbf{v}+\eta\mathbf{j}^2+\Phi, \tag{14}$$

$$\frac{\partial\Psi}{\partial t}=-E_z, \tag{15}$$

$$\frac{\partial B_z}{\partial t}=-\nabla\times\mathbf{E}_p. \tag{16}$$

Here, $\mathbf{j}$, $\mathbf{E}$, $\mathbf{B}$, Φ, and e_{ij} are, respectively, given by

$$\mathbf{j}=j_z\hat{\mathbf{z}}+\mathbf{j}_p=-\hat{\mathbf{z}}\nabla^2\Psi+\nabla B_z\times\hat{\mathbf{z}}, \tag{17}$$

$$\mathbf{E}=E_z\hat{\mathbf{z}}+\mathbf{E}_p=-\mathbf{v}\times\mathbf{B}+\eta\mathbf{j}, \tag{18}$$

$$\mathbf{B}=B_z\hat{\mathbf{z}}+\nabla\Psi\times\hat{\mathbf{z}}, \tag{19}$$

$$\Phi=2\nu\left(e_{ij}e_{ij}-\frac{1}{3}(\nabla\cdot\mathbf{v})^2\right), \tag{20}$$

$$e_{ij}=\frac{1}{2}\left(\frac{\partial v_i}{\partial x_j}+\frac{\partial v_j}{\partial x_i}\right). \tag{21}$$

Downloaded 12 Jun 2009 to 133.75.139.172. Redistribution subject to AIP license or copyright; see http://pop.aip.org/pop/copyright.jsp

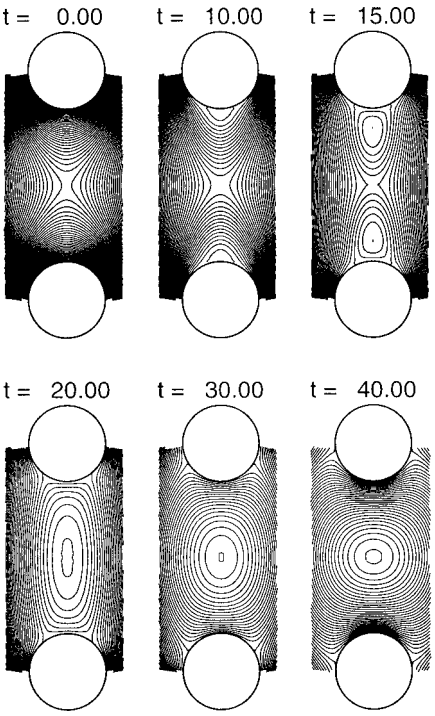

FIG. 4. Contour plots of poloidal flux at different time steps in the MHD simulation with a constant resistivity ($\eta=1\times10^{-3}$).

The suffix p denotes a poloidal (x,y) component of a vector. Velocity $\mathbf{v}$ is set to be zero on the boundaries. We have used a perfect conductor for the outer boundary, while $\mathbf{E}_p=0$ and $E_z=0.01$ on the inner boundaries that correspond to the FC coil surfaces. All of physical quantities are normalized by the typical length $L_x=1$, a characteristic poloidal magnetic field $B_{p0}=\Psi_0/L_x=1$, and the initial density $\rho_0=1$. The Alfvén velocity V_{A0} given by B_{p0} and ρ_0 is equal to 1. Time is measured by the Alfvén transit time $\tau_A=L_x/V_{A0}$. The initial pressure is set to be $p=0.2$. Viscosity ν and ratio of the specific heats Γ are, respectively, $\nu=1\times10^{-3}$ and $\Gamma=5/3$.

First, we have performed the MHD simulations with a constant resistivity η, adding infinitesimal random perturbations of $\mathbf{v}$ at $t=0$. Starting from the initial condition with the boundary condition given above, Eqs. (12)–(16) are integrated in time by the fourth-order Runge–Kutta–Gill method.[15,16] Spatial derivatives are calculated by the second-order finite difference. Figure 4 shows contour plots of Ψ at different time steps for $\eta=1\times10^{-3}$, where only an area nearby FC coils is plotted for clarity. The Lundquist number S is equal to the inverse of η, that is, 10^3 in this case. Total grid points of 101×141 including FC coils are employed in this simulation, while a convergence check using finer grid points of 201×281 gives the same results. Two circles on top and bottom of each figure represent the FC coil surfaces. Decreasing of Ψ_0 on the FC coil surfaces causes a plasma flow which drives magnetic reconnection at the X-point, while an induction current is enhanced around the FC coils. The increased current detaches a part of the ''private'' flux from each FC coil surface, and forms magnetic islands (see a plot at $t=15\tau_A$). The formation process of the islands is the same as that of the S-1 spheromak using a FC coil.[12,17] Then,

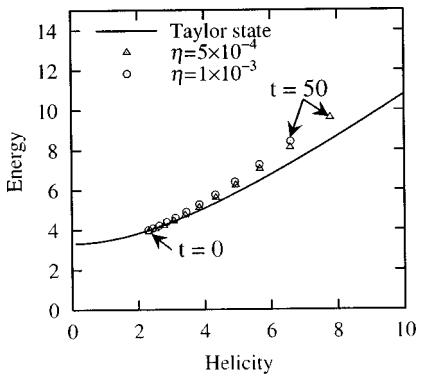

FIG. 5. Evolution of the magnetic energy and helicity. Solid line shows the Taylor state. Marks representing simulation results are plotted at every $5\tau_A$.

the magnetic islands collide with each other, and merge into a larger one. As Ψ_0 is decreased further, the single island grows more and covers the whole system, as is predicted by the Taylor state analysis in the last section. Through several simulations with different η from 5×10^{-4} to 1×10^{-2}, we have found common features in their time evolutions, such as detachment of the ''private'' flux, merging of the two islands, and growth of the merged island.

In Fig. 5 we have plotted the normalized magnetic energy versus the helicity resulted from the MHD simulations with $\eta=1\times10^{-3}$ and 5×10^{-4}. For $\eta=5\times10^{-4}$, we have used 201×281 grid points. A solid line in the figure shows the Taylor state given by Eq. (7), while marks represent the simulation results at every $5\tau_A$. Here, the energy E and helicity H are, respectively, normalized by $(\Psi_0/L_x)^2$ and Ψ_0^2/L_x. One finds that, following the Taylor state, the normalized energy and helicity are increased as Ψ_0 is decreased

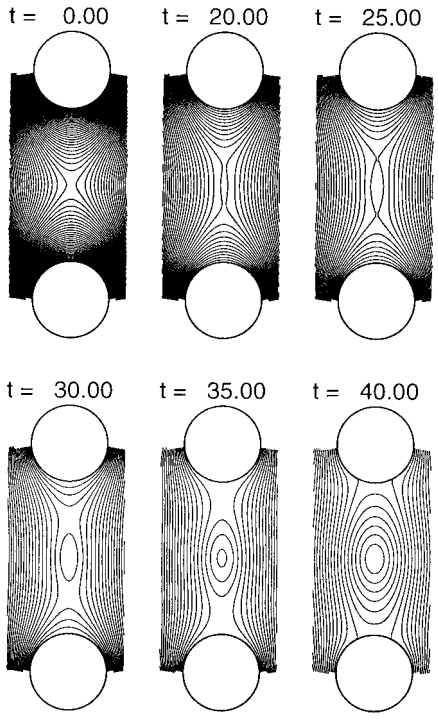

FIG. 6. Same as Fig. 4 but with a nonuniform resistivity.

Downloaded 12 Jun 2009 to 133.75.139.172. Redistribution subject to AIP license or copyright; see http://pop.aip.org/pop/copyright.jsp

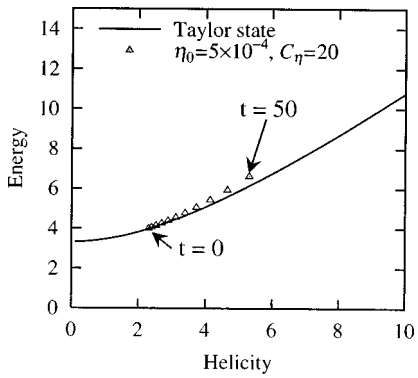

FIG. 7. Same as Fig. 5 but with a nonuniform resistivity.

in time. Thus, the magnetic island appears and grows. It is also seen that the time evolution of E and H for smaller η is closer to the Taylor state.

The above simulation result explains the growth of a magnetic island found in the MRX cohelicity discharge. In the experiment, however, the island appears in a central plasma region apart from the FC coil surfaces. Namely, it is created when a mean poloidal flux remains in the ''private'' regions. On the other hand, in the above simulation, two islands are formed by reconnection on the FC coil surfaces. This is because the large induction current flows around the FC coils due to the constant η. It is, however, considered that η might be larger nearby the FC coils than in the central region because of higher impurity density. Thus, we have performed simulations with an inhomogeneous η such as

$$\eta=\eta_0[1+C_\eta \exp\{-(r-r_c)^2/r_c^2\}], \tag{22}$$

where r and r_c denote a distance from a center of the nearest FC coil and its radius. In Fig. 6 we show contour maps of Ψ at different time steps for $\eta_0=5\times10^{-4}$ and $C_\eta=20$. As seen in the figures a small island appears in the current layer accompanying reconnection, and gradually becomes larger while Ψ_0 is reduced. The formation process of the magnetic island is consistent with the MRX one. We have also found that the induction current mainly flows in the central region, where the island is created, rather than around the FC coils because of the inhomogeneous η profile. In addition, it is confirmed that, for smaller C_η such as $C_\eta=10$ with $\eta_0=5\times10^{-4}$, magnetic islands appear on the FC coil surfaces as seen in Fig. 4, which suggests the importance of the nonuniform η in the island formation.

Figure 7 shows the normalized helicity and energy obtained by the simulation in Fig. 6. Even with the larger resistivity near the FC coil surfaces, the helicity and energy are increased along the Taylor state, although the increasing rate is smaller than the constant η cases in Fig. 5. Thus, it is suggested that the global property of island growth could be explained by the Taylor's theory, whereas the resistivity influences on the detail process of island formation in an early phase and its time scale.

IV. CONCLUDING REMARKS

In this study we have investigated the magnetic island formation in the MRX discharge. The Taylor state analysis shows that two types of solutions with and without a magnetic island belong to the lowest branch which continues from $\mu=0$ to $|\mu|=\lambda_1$. Quasistatic transition of the field configuration along the branch can explain growth of the magnetic island during the poloidal flux is ''pulled'' into the FC coils, since the normalized helicity, namely, μ is increased by decreasing the PF coil currents. It is also deduced from the Taylor state analysis that no magnetic island is formed in the counterhelicity injection. While the theoretical analysis gives an understanding on the global evolution of the system, a detailed process for appearance of the island needs a more realistic consideration, that is, the nonuniform resistivity. The inhomogeneous resistivity such as Eq. (22) enables the induction current to concentrate in the central plasma region rather than around the FC coils, and thus, to form the magnetic island apart from the coil surfaces. The simulation result using the MHD model with the nonuniform resistivity can successfully explain the cohelicity injection of MRX in the ''pulling'' operation mode.

ACKNOWLEDGMENTS

One of the authors (T.-H.W.) would like to thank S. C. Jardin, R. M. Kulsrud, S. Kida, R. Horiuchi, K. Kusano, and A. Kageyama for their fruitful comments and discussions. Numerical computations in this study are performed on the NIFS MISSION System (Man-Machine Interactive System for Simulation). This work is partially supported by the Grants-in-Aid of Ministry of Education, Science, Culture, and Sports in Japan (09780445, 10898016, 0987890, and 10044105) and the exchange program of the Joint Institute for Fusion Theory (97JF1-14).

[1] E. N. Paker, in *Cosmical Magnetic Fields* (Clarendon, Oxford, 1979).
[2] T. Sato and T. H. Hayashi, Phys. Fluids **22**, 1189 (1979); H. Amo, T. Sato, A. Kageyama, and the Complexity Simulation Group, Phys. Rev. E **51**, 3838 (1995).
[3] D. Biskamp, Phys. Rep. **237**, 179 (1993).
[4] T. Sato and K. Kusano, Phys. Rev. Lett. **54**, 808 (1985).
[5] M. Yamada, Y. Ono, A. Hayakawa, M. Katsurai, and F. W. Perkins, Phys. Rev. Lett. **65**, 721 (1990).
[6] T.-H. Watanabe, T. Sato, and T. Hayashi, Phys. Plasmas **4**, 1297 (1997).
[7] M. Yamada, H. Ji, S. Hsu, T. Carter, R. Kulsrud, N. Bretz, F. Jobes, Y. Ono, and E. Perkins, Phys. Plasmas **4**, 1936 (1997).
[8] M. Yamada, H. Ji, T. A. Carter, S. C. Hsu, R. M. Kulsrud, N. L. Bretz, F. C. Jones, Y. Ono, M. Katsurai, T.-H. Watanabe, T. Sato, and T. Hayashi, in *Proceedings of the 16th International Conference on Fusion Energy*, Montreal, 1996 (International Atomic Energy Agency, Vienna, 1997), Vol. 2, p. 253.
[9] M. Yamada, H. Ji, S. Hsu, T. Carter, R. Kulsrud, Y. Ono, and F. Perkins, Phys. Rev. Lett. **78**, 3117 (1997).
[10] D. D. Schnack (private communication, 1998).
[11] J. B. Taylor, Phys. Rev. Lett. **33**, 1139 (1974).
[12] S. C. Jardin and W. Park, Phys. Fluids **24**, 679 (1981).
[13] J. B. Taylor, Rev. Mod. Phys. **58**, 741 (1986).
[14] T. H. Jensen and M. S. Chu, Phys. Fluids **27**, 2881 (1984).
[15] R. Horiuchi and T. Sato, Phys. Fluids B **1**, 581 (1989).
[16] K. Watanabe and T. Sato, J. Geophys. Res. **95**, 75 (1990).
[17] M. Yamada, H. P. Furth, W. Hsu, A. Janos, S. Jardin, M. Okabayashi, J. Sinnis, T. H. Stix, and K. Yamazaki, Phys. Rev. Lett. **46**, 188 (1981).

Downloaded 12 Jun 2009 to 133.75.139.172. Redistribution subject to AIP license or copyright; see http://pop.aip.org/pop/copyright.jsp